Supplementary Material

Airborne Strapdown Gravity Survey of Sos Enattos Area (NE Sardinia, Italy): Insights into Geological and Geophysical Characterization of the Italian Candidate Site for the Einstein Telescope

Filippo Muccini [1], Filippo Greco [2], Luca Cocchi [1,*], Maria Marsella [3], Antonio Zanutta [4], Alessandra Borghi[5], Matteo Cagnizi [3], Daniele Carbone [2], Mauro Coltelli [2], Danilo Contrafatto [2], Peppe Junior Valentino D'Aranno [3], Luca Frasca [2], Alfio Alex Messina [2], Luca Timoteo Mirabella [2], Monia Negusini [6] and Eleonora Rivalta [7]

[1] Istituto Nazionale di Geofisica e Vulcanologia, Via di Vigna Murata 605, 00143 Roma, Italy; filippo.muccini@ingv.it
[2] Istituto Nazionale di Geofisica e Vulcanologia, Piazza Roma, 2, 95125 Catania, Italy; filippo.greco@ingv.it (F.G.); daniele.carbone@ingv.it (D.C.); mauro.coltelli@ingv.it (M.C.); danilo.contrafatto@ingv.it (D.CO.); luca.frasca@ingv.it (L.F.); alfio.messina@ingv.it (A.A.M.); luca.mirabella@ingv.it (L.T.M.)
[3] Department of Civil, Environmental and Building Engineering (DICEA), Università degli Studi di Roma 'La Sapienza', 00184 Roma, Italy; maria.marsella@uniroma1.it (M.M.); matteo.cagnizi@uniroma1.it (M.CA.); peppejuniorvalentino.daranno@uniroma1.it (P.D.)
[4] Department of Civil, Chemical, Environmental and Materials Engineering (DICAM), Alma Mater Studiorum, Università di Bologna, Viale Risorgimento 2, 40136 Bologna, Italy; antonio.zanutta@unibo.it
[5] Istituto Nazionale di Geofisica e Vulcanologia, Viale Berti Pichat 6/2, 40127 Bologna, Italy; alessandra.borghi@ingv.it
[6] Istituto Nazionale di Astrofisica, Istituto di Radioastronomia, Via P. Gobetti 101, 40129 Bologna, Italy; negusini@ira.inaf.it
[7] Department of Physics and Astronomy (DIFA), Alma Mater Studiorum, Universita di Bologna, Viale Berti Pichat, 8, 40126 Bologna, Italy; eleonora.rivalta@unibo.it
* Correspondence: luca.cocchi@ingv.it; Tel.: +39-0187794408

Supplementary Text:

Noise Level floor estimation

To assess the residual uncertainty associated with instrumental and vibrational noise, we estimated the noise level floor for each flight line. This estimation was based on the power spectral density (PSD) of the filtered gravity signal, focusing on the frequency band between 0.05 and 0.2 Hz, where the spectral content is expected to be dominated by noise rather than geophysical signal. This approach follows established practices in inertial gravity, where PSD analysis allows for the separation of stochastic noise from deterministic signals and is considered effective in quantifying the uncertainty of navigation-derived gravity estimates [52].

We computed the PSD for each flight line and estimated the noise level in terms of mGal/√Hz. Figure S1 shows the PSD of Line 14, including its estimated noise level. Based on the distribution of noise values across all lines, we calculated the mean and standard deviation to characterize overall noise performance. A graphical representation of this distribution is provided in the histogram plot shown in Figure S2.

Supplementary Figures

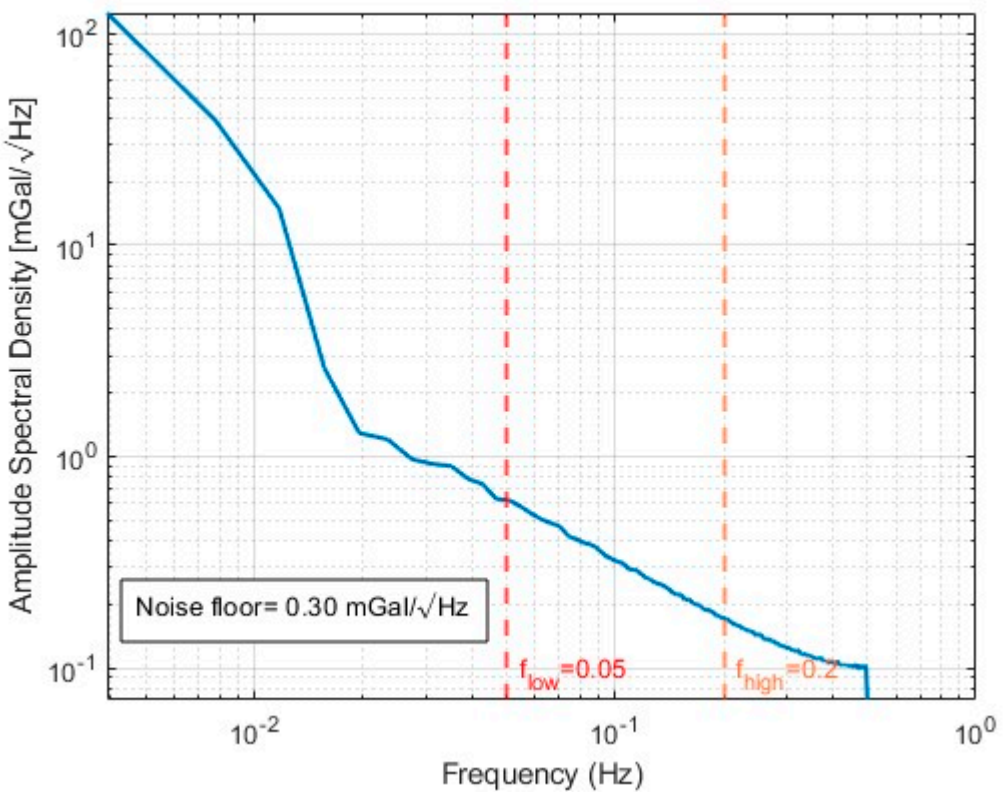


Figure S1. Power Spectra density of Line number 10. Estimated Noise value 0.30 mGal/√Hz in the frequency range of 0.05 (F_{low}) and 0.2 (F_{high}).

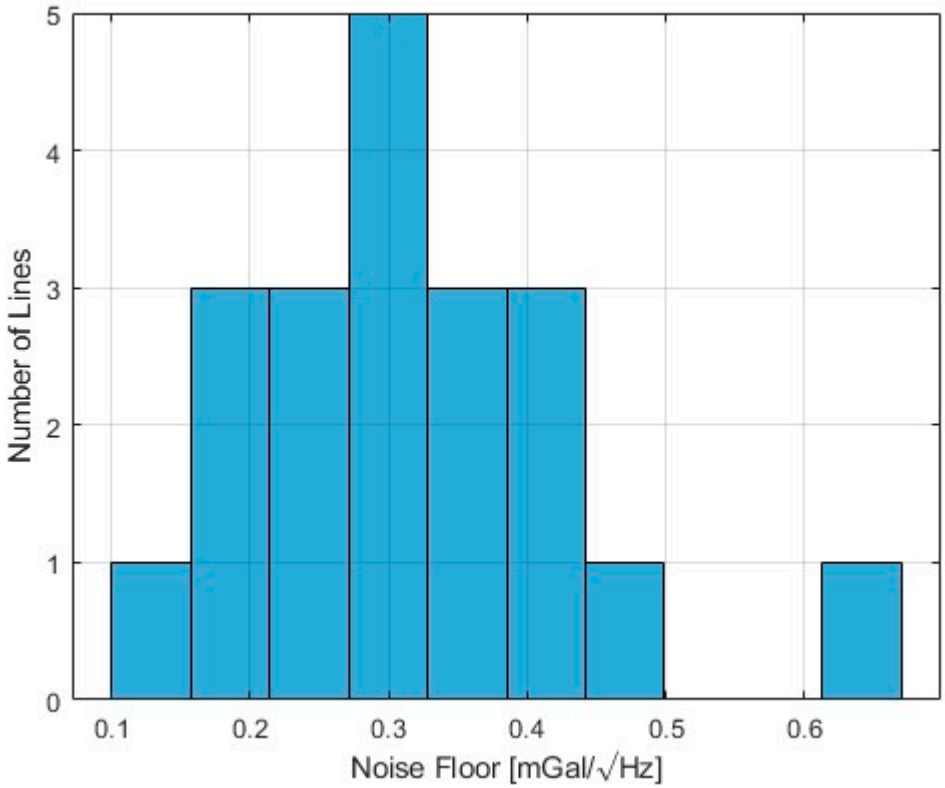


Figure S1. Histogram of noise floor levels across all gravity survey lines. The distribution follows an approximately Gaussian shape centered around the mean value of 0.3 mGal/√Hz, with a standard deviation of approximately 0.12 mGal/√Hz. All lines exhibit noise levels below 0.5 mGal/√Hz, except for a single outlier at 0.669 mGal/√Hz.

Table S1. Cross over error estimation of the airborne gravity data in the Sos Enattos region

X Utm	Y Utm	Line	Gradient Line	Levelled Value	Tie Line	Gradient Tie Line	Tie Value	Cross over error
549484.3	4487113.4	L1	0.2	74.05	T1	0.2	69	-5.1
549488.5	4493283.5	L1	0.1	61.23	T2	0.2	57.7	-3.49
549492.1	4480903.3	L1	0.3	57.82	T3	0.3	53.5	-4.3
547497.8	4487109.1	L2	0.2	60.88	T1	0.2	61.8	0.92
547513.4	4493310.1	L2	0	45.92	T2	0.3	49.1	3.21
547507.7	4480902.3	L2	0.4	66.98	T3	0.5	67.6	0.67
545524.5	4487092.9	L3	0.1	58.38	T1	0.3	54.6	-3.8
545495.6	4493311.7	L3	0	44.25	T2	0.2	40.1	-4.2
545501.7	4480907.3	L3	0.2	79.23	T3	0.2	74.3	-4.92
543507.2	4487104.8	L4	0.1	49.24	T1	0.2	45.5	-3.69
543519.1	4493296	L4	0	34.95	T2	0.1	33.8	-1.11
543514.6	4480901.7	L4	0.1	63.95	T3	0.4	64	0.05
541513.6	4487070.4	L5	0.1	40.8	T1	0	43	2.23
541522.5	4493299.2	L5	0	39.1	T2	0.2	35.1	-4.03
541510	4480914.1	L5	0	55.18	T3	0.1	56.6	1.45

539484.4	4487098.1	L6	0.1	50.96	T1	0.2	46	-4.95
539508	4493301.3	L6	0.1	54.18	T2	0.6	49.2	-4.97
539516.5	4480923.9	L6	0.1	58.26	T3	0.1	54.6	-3.61
538820.1	4487096.8	L7	0.1	50.65	T1	0.3	48.5	-2.1
538819.5	4493292.1	L7	0.1	59.53	T2	0.5	55.3	-4.22
538816.9	4480921	L7	0.1	55.31	T3	0.1	54	-1.3
537512	4487104	L8	0.1	51.69	T1	0.3	54.8	3.11
537503.9	4493282.1	L8	0.2	60.48	T2	0.3	64	3.53
537500.2	4480908.8	L8	0.1	48.37	T3	0	53.3	4.9
535511.5	4487103.3	L9	0.2	62.28	T1	0.3	65.1	2.79
535517.3	4493311.1	L9	0.3	70.06	T2	0.1	68.7	-1.33
535515.5	4480918.3	L9	0.2	51.45	T3	0.1	54.5	3
533509.2	4468649.8	L10	0	21	L19	0.1	24	2.99
533514.8	4487097.7	L10	0.2	67.61	T1	0	68.7	1.09
533510.8	4493308.8	L10	0.3	68.94	T2	0.2	73.7	4.73
533526.9	4480915.4	L10	0.2	54.23	T3	0.1	57.5	3.31
517523.8	4487103.1	L11	0	57.2	T1	0.1	57.6	0.38
517522.6	4493300.8	L11	0.1	60.33	T2	0.1	59.8	-0.49
517527.2	4480911.2	L11	0.1	53.54	T3	0.1	54.8	1.31
519505.1	4487091.1	L12	0	62.56	T1	0	59.5	-3.1
519492.2	4493288	L12	0.2	64.58	T2	0	61.7	-2.85
519507.1	4480901.1	L12	0.1	62.14	T3	0.2	58.5	-3.66
521540	4487104	L13	0.2	58.42	T1	0	58.8	0.41
521523	4493301.5	L13	0.1	65.9	T2	0	61.2	-4.69
521524	4480903.1	L13	0.1	57.73	T3	0.1	62.6	4.86
523502.2	4487098.7	L14	0.1	63.84	T1	0.2	62	-1.82
523529.7	4493307.9	L14	0.3	68.44	T2	0.2	64.4	-4.06
523505.8	4480902.5	L14	0.1	67.83	T3	0	63.4	-4.39
525508.5	4487100.2	L15	0	62.02	T1	0.1	66	4
525520.7	4493303.1	L15	0.2	66.54	T2	0.2	71	4.5
525530.4	4480910.6	L15	0.1	69.32	T3	0.3	68.1	-1.2
527512.2	4487103.6	L16	0.1	65.9	T1	0.1	69.3	3.43
527502.6	4493305.3	L16	0.1	70.24	T2	0	74.4	4.17
527512.1	4480931.5	L16	0.2	70.42	T3	0.1	74.6	4.13
529508.5	4487087.6	L17	0.1	67.97	T1	0	71.7	3.71
529511.1	4493300.5	L17	0.2	69.95	T2	0	74.9	4.97
529498.2	4480934.4	L17	0	67.28	T3	0.3	71	3.7
531504	4487091.3	L18	0.2	64.11	T1	0.1	68.7	4.64
531512	4493291.3	L18	0.3	72	T2	0	76.3	4.32
531505	4480911.7	L18	0.2	59.51	T3	0.2	62.2	2.67
533509.2	4468649.8	L19	0.1	24	L10	0	21	-2.99
533497.1	4487098	L19	0.3	67.83	T1	0	68.7	0.86
533521.3	4493308.8	L19	0.3	68.67	T2	0.2	73.6	4.98
533506.1	4480915.4	L19	0.2	55.75	T3	0.1	57.6	1.82